Semnan University

Unsteady free convection flow between two vertical plates with variable temperature and mass diffusion

Sanatan Das[1], Rabindera Nas Jana[2] and Ali Chamkha*[3]

[1]*Department of Mathematics, University of Gour Banga, Malda 732 103, India*
[2]*Department of Applied Mathematics, Vidyasagar University, Midnapore 721 102, India*
[3]*Manufacturing Engineering Department, Prince Mohammad Bin Fahd University, P.O. Box 1664, Al-Khobar 31952, Saudi Arabia*

A B S T R A C T

The unsteady free convection flow between two long vertical parallel plates with variable temperature and mass diffusion in the presence of the thermal radiation has been presented. The governing dimensionless coupled linear partial differential equations on the flow are solved by using the Laplace transform technique. The Exact solutions have been obtained for the fluid velocity, temperature and the mass concentration. The Representative numerical results for the fluid velocity, temperature, mass concentration and the shear stresses at the plate are presented graphically for the various pertinent flow parameters such as the radiation parameter, buoyancy forces, Schmidt number and time and studied in detail. The study shows that these parameters have significant impact on the velocity, temperature, mass concentration and the shear stresses at the plates.

1. Introduction

The Natural convection has been analyzed extensively by many researchers. Sometimes, along with the free convection currents caused by difference in temperature, the flow is also affected by the differences in concentration or material constitution. There are many situations where the convection heat transfer phenomena are accompanied by mass transfer also. When mass transfer takes place in a fluid ??, the mass is transferred purely by molecular diffusion resulting from concentration gradients. For low concentration of the mass in the fluid and low mass transfer rates, the convective heat and mass transfer processes are similar in nature. A number of investigations have already been carried out with combined heat and mass transfer under the assumption of different physical situations. The illustrative examples of mass transfer can be found in the book of Cussler [1]. The Free convection resulting from the combined thermal and mass buoyancy forces has received significant attention of engineers and scientists due to many applications in engineering and technological processes. The significant applications include the thermal processes in the vertical mounting board electronic components, channel-chimney systems, thermal comfort dynamics in building services, nuclear reactor thermal hydraulics and frost formation. The Theoretical investigation of unsteady free convection flow due to heat and mass transfer in vertical parallel plate channel received less attention than numerical investigations. It is well known that the effects of radiation on free convection flow problems have become more important industrially. Many engineering processes

Corresponding author: Ali Chamkha, Manufacturing Engineering Department, Prince Mohammad Bin Fahd University, P.O. Box 1664, Al-Khobar 31952, Saudi Arabia

occur at high temperatures, the knowledge of radiative heat transfer plays significant role in the design of equipments. Nuclear power plants, gas turbines and various propulsion devices for aircraft, missiles, satellites and space vehicles are examples of such engineering processes. At high operating temperature, the radiation effect can be quite significant. The study of free convection flow with radiative heat and mass transfer also plays an important role in biological sciences. The Effects of various parameters on human body can be studied and appropriate suggestions can be given to the persons working in hazardous areas with noticeable effects of magnetism and heat variation.

The results of theoretical analysis can be served as a guide for both experimental and numerical investigations. The Natural convection heat and mass transfer in a vertical channel consisting of two vertical parallel plates, one porous and the other non-porous, with opposing buoyancy forces was studied numerically by using finite difference method and experimentally by Lee et al. [2]. They observed that the mass transfer from the porous wall resulted in a downward flow while the heat transfer from the non-porous wall resulted in an opposing upward flow. The effects of latent heat transfer associated with the thin liquid film vaporization on the heat transfer in natural convection flows driven by the combined buoyancy forces of thermal and mass diffusion between vertical parallel plates by using an implicit finite difference method has been studied by Yan et al.[3]. A numerical analysis for developing laminar flow between vertical parallel plates with natural convection heat and mass transfer for uniform wall temperature and the concentration have been presented by Nelson and Wood [4]. Nelson and Wood [5] have also obtained an analytical solution for fully developed heat and mass transfer natural convection flow between vertical parallel plates with asymmetric boundary conditions. Yan and Lin [6] have carried out a numerical analysis to investigate the effects of latent heat transfer and finite liquid film evaporation on the channel wall and on the natural convection heat and mass transfer. They specifically presented the results for ethanol film evaporation and water film evaporation. Yan and Lin [7] have also carried out a numerical study to investigate the evaporative cooling of liquid falling film through interfacial heat and mass transfer in natural convection channel flows. The results for heat and mass transfer rates have specifically presented for ethanol film evaporation and the predicted results were also contrasted with the experimental results obtained by Yan and Lin [8]. Desrayaud and Lauriat [9] have made a numerical study to investigate buoyancy induced by heat and mass transfer analogy for condensation of humid air flowing in a vertically heated channel based on thin-film assumptions. A finite-difference analysis has been presented by Salah El-Din [10] to investigate the effect of the thermal and mass buoyancy forces on the development of laminar mixed convection between two vertical parallel plates with uniform heat and mass fluxes. The closed-form analytic solutions have been derived by Cheng [11] to examine the effect of the vortex viscosity parameter and the buoyancy ratio on the fully developed natural convection heat and mass transfer of a micropolar fluid in a vertical channel with asymmetric wall temperatures and concentrations. Narahari [12] has presented an analytical study by using the Laplace transform technique for the transient free convection flow of a viscous incompressible fluid between two vertical parallel plates in the presence of constant temperature and mass diffusion. The natural convection due to heat and mass transfer between vertical parallel plates has not received much attention despite important applications in many engineering systems.

The main purpose of the present investigation is to study the unsteady free convection flow of an optically dense viscous incompressible fluid between two long vertical parallel plates with variable temperature and mass diffusion in the presence of thermal radiation. Assume that the flow is laminar and the fluid is gray absorbing-emitting radiation but no scattering medium. It is considered that the fluid to be optically thick instead of optically thin in this problem. Rosseland diffusion approximation is used to describe the radiative heat flux in the energy equation. The Closed form solutions of the initial and boundary value problems that govern the flow are obtained by means of the Laplace transform technique. The effects of pertinent flow parameters on the fluid velocity, temperature and mass concentration profiles are presented graphically and the physical aspects of the problem are discussed.

2. Formulation of the problem and its solutions

Consider the unsteady free convection flow of a viscous incompressible fluid between two long vertical parallel plates separated by a distance h. Choose a Cartesian coordinates system with the x - axis taken along one of the plates of the channel and the y -axis normal to the plates (See Fig. 1). Initially, at time $t \leq 0$, both the plates and the fluid are assumed to be at the same temperature T_h and concentration C_h. At time $t > 0$, the temperature and mass concentration at the plate at $y = 0$ have been raised to $T_h + (T_0 - T_h)\dfrac{t}{t_0}$ and $C_h + (C_0 - C_h)\dfrac{t}{t_0}$, respectively, T_0 and C_0 the constant temperature and mass concentration and t_0 the characteristic time while that of the other plate at $y = h$ continues to remain at the initial temperature T_h and mass concentration C_h. The flow is considered to be laminar without any pressure gradient in the flow direction. It is also assumed that the radiative heat flux in the x - direction is negligible as compared to that in the y - direction. The density is assumed to be linearly dependent on mass concentration and temperature buoyancy forces in the equations of motion. This approximation is exact enough for both dropping liquid and gases at small values of the temperature and diffusion differences. As the plates are long along x direction infinitely, the velocity and temperature fields are functions of y and t only.

It should be noted that the temperature and concentration differences were small enough in the analyzed heat and mass transfer process. Therefore, use of the Boussinesq approximation and analogy between heat and mass transfer processes is pertinent. The unsteady natural convection flow of a radiating fluid, under usual Boussinesq approximation, is governed by the following equations:

$$\frac{\partial u}{\partial t} = \nu \frac{\partial^2 u}{\partial y^2} + g\beta(T - T_\infty) + g\beta^*(C - C_\infty), \qquad (1)$$

$$\rho c_p \frac{\partial T}{\partial t} = k \frac{\partial^2 T}{\partial y^2} - \frac{\partial q_r}{\partial y}, \qquad (2)$$

$$\frac{\partial C}{\partial t} = D \frac{\partial^2 C}{\partial y^2}, \qquad (3)$$

where u is the fluid velocity in the x -direction, T the temperature and C the mass concentration of the fluid, g the acceleration due to gravity, β
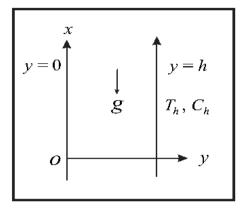

Fig. 1: Geometry of the problem

the coefficient of thermal expansion, β^* coefficient of volumetric expansion due to concentration change, ν the kinematic viscosity, ρ the fluid density, k the thermal conductivity, c_p the specific heat at constant pressure, D mass diffusivity and q_r the radiative heat flux. The heat due to viscous dissipation is neglected for small velocities in the energy equation (2).

The study of combined heat and mass transfer problems are important in many processes such as drying, evaporation at the surface of water body, energy transfer in a wet cooling tower, solidification of binary alloy, dispersion of dissolved materials, drying and dehydration operations in chemical food processing plants and combustion of atomized liquid fuels.

The initial and boundary conditions are

$t \leq 0 : u = 0, \ T = T_h, \ C = C_h \ \text{for all} \ 0 \leq y \leq h,$

$t > 0 : u = 0, \ T = T_h + (T_0 - T_h)\dfrac{t}{t_0}, \ C = C_h + (C_0 - C_h)\dfrac{t}{t_0} \ \text{at} \ y = 0, \qquad (4)$

$t > 0 : u \rightarrow 0, \ T = T, \ C = C \ \text{at} \ y = h$

In order to simplify the physical problem, the optically thick radiation limit is considered in the present analysis. The radiative heat flux for an optically thick fluid can be found from Rosseland approximation [13] and its formula is derived from the diffusion concept of radiative heat transfer in the following way:

$$q_r = -\frac{4\sigma}{3k^*} \frac{\partial T^4}{\partial y}, \qquad (5)$$

where σ is the Stefan-Boltzman constant and k^* the spectral mean absorption coefficient of the medium. It should be noted that by using the Rosseland approximation we limit our analysis to optically thick

fluids. If the temperature differences within the flow are sufficiently small, then the equation (5) can be linearized by expanding T^4 into the Taylor series about the temperature T_h and neglecting higher order terms to give

$$T^4 \approx 4T_h^3 T - 3T_h^4. \tag{6}$$

by using the equations (5) and (6), equation (2) becomes

$$\rho c_p \frac{\partial T}{\partial t} = k \frac{\partial^2 T}{\partial y^2} + \frac{16\sigma T_h^3}{3k^*} \frac{\partial^2 T}{\partial y^2}. \tag{7}$$

By Introducing the dimensionless variables

$$\eta = \frac{y}{h}, \ \tau = \frac{tv}{h^2}, \ u_1 = \frac{uh}{v}, \ \theta = \frac{T - T_h}{T_0 - T_h}, \ \phi = \frac{C - C_h}{C_0 - C_h}, \tag{8}$$

equations (1), (7) and (3) become

$$\frac{\partial u_1}{\partial \tau} = \frac{\partial^2 u_1}{\partial \eta^2} + Gr\theta + Gc\phi, \tag{9}$$

$$\alpha \frac{\partial \theta}{\partial \tau} = \frac{\partial^2 \theta}{\partial \eta^2}, \tag{10}$$

$$Sc \frac{\partial \phi}{\partial \tau} = \frac{\partial^2 \phi}{\partial \eta^2}, \tag{11}$$

where $R = \frac{kk^*}{4\sigma T_h^3}$ is the radiation parameter,

$Pr = \frac{\rho v c_p}{k}$ the Prandtl number, $Gr = \frac{g\beta(T_0 - T_h)h^3}{v^2}$

the Grashof number, $Gc = \frac{g\beta^*(C_0 - C_h)h^3}{v^2}$ the mass

Grashof number, $Sc = \frac{v}{D}$ Schmidt number and

$\alpha = \frac{3PrR}{3R + 4}$.

The corresponding initial and the boundary conditions are

$\tau \leq 0 : u_1 = 0, \ \theta = 0, \ \phi = 0, \ \text{for all } 0 \leq \eta \leq 1$

$\tau > 0 : u_1 = 0, \ \theta = \tau, \ \phi = \tau \ \text{at } \eta = 0,$ (12)

$\tau > 0 : u_1 = 0, \theta = 0, \ \phi = 0 \ \text{at } \eta = 1.$

by using Laplace transformation, equations (9) - (11) become

$$s\bar{u}_1 = \frac{\partial^2 \bar{u}_1}{\partial \eta^2} + Gr\bar{\theta} + Gc\bar{\phi}, \tag{13}$$

$$s\alpha\bar{\theta} = \frac{\partial^2 \bar{\theta}}{\partial \eta^2}, \tag{14}$$

$$sSc\bar{\phi} = \frac{\partial^2 \bar{\phi}}{\partial \eta^2}, \tag{15}$$

where

$$\bar{u}_1(\eta, s) = \int_0^\infty u_1(\eta, \tau)e^{-s\tau}\, d\tau, \ \bar{\theta}(\eta, s) = \int_0^\infty \theta(\eta, \tau)e^{-s\tau}\, d\tau,$$

$$\bar{\phi}(\eta, s) = \int_0^\infty \phi(\eta, \tau)e^{-s\tau}\, d\tau. \tag{16}$$

The corresponding boundary conditions for $\bar{u}_1$, $\bar{\theta}$ and $\bar{\phi}$ are

$\bar{u}_1 = 0, \ \bar{\theta} = \frac{1}{s^2}, \ \bar{\phi} = \frac{1}{s^2} \ \text{at } \eta = 0,$ (17)

$\bar{u}_1 = 0, \ \bar{\theta} = 0, \ \bar{\phi} = 0 \ \text{at } \eta = 1$

The solution of the equations (13)- (15) subject to the boundary conditions (17) are given by

$$\bar{\theta}(\eta, s) = \frac{1}{s^2} \sum_{n=0}^\infty \left(e^{-a\sqrt{s\alpha}} - e^{-b\sqrt{s\alpha}} \right), \tag{18}$$

$$\bar{\phi}(\eta, s) = \frac{1}{s^2} \sum_{n=0}^\infty \left(e^{-a\sqrt{sSc}} - e^{-b\sqrt{sSc}} \right), \tag{19}$$

$$\bar{u}_1(\eta, s) = \frac{Gr(Sc-1) + Gc(\alpha-1)}{(\alpha-1)(Sc-1)s^3} \sum_{n=0}^\infty \left(e^{-a\sqrt{s}} - e^{-b\sqrt{s}} \right)$$

$$- \frac{Gr}{(\alpha-1)s^3} \sum_{n=0}^\infty \left(e^{-a\sqrt{s\alpha}} - e^{-b\sqrt{s\alpha}} \right) \tag{20}$$

$$- \frac{Gc}{(Sc-1)s^3} \sum_{n=0}^\infty \left(e^{-a\sqrt{sSc}} - e^{-b\sqrt{sSc}} \right)$$

where $a = 2n + \eta$ and $b = 2n + 2 - \eta$.

The inverse Laplace transforms of the equations (18)-(19) give the solution for the velocity, temperature and concentration distributions as

$$\theta(\eta, \tau) = \sum_{n=0}^\infty \left[f_1(a\sqrt{\alpha}, \tau) - f_1(b\sqrt{\alpha}, \tau) \right], \tag{21}$$

$$\phi(\eta, \tau) = \sum_{n=0}^\infty \left[f_1(a\sqrt{Sc}, \tau) - f_1(b\sqrt{Sc}, \tau) \right], \tag{22}$$

$$u_1(\eta, \tau) = \frac{Gr(Sc-1) + Gc(\alpha-1)}{(\alpha-1)(Sc-1)} \sum_{n=0}^\infty \left[f_2(a, \tau) - f_2(b, \tau) \right]$$

$$- \frac{Gr}{\alpha-1} \sum_{n=0}^\infty \left[f_2(a\sqrt{\alpha}, \tau) - f_2(b\sqrt{\alpha}, \tau) \right] \tag{23}$$

$$- \frac{Gc}{Sc-1} \sum_{n=0}^\infty \left[f_2(a\sqrt{Sc}, \tau) - f_2(b\sqrt{Sc}, \tau) \right],$$

where

$$f_1(\xi, \tau) = \left(\tau + \frac{1}{2}\xi^2 \right) erfc\left(\frac{\xi}{2\sqrt{\tau}} \right) - \xi\sqrt{\frac{\tau}{\pi}}\, e^{-\frac{\xi^2}{4\tau}},$$

$$f_2(\xi, \tau) = \frac{1}{2}\left(\tau^2 + \tau\xi^2 + \frac{1}{12}\xi^4 \right) erfc\left(\frac{\xi}{2\sqrt{\tau}} \right) \tag{24}$$

$$- \frac{1}{6}\sqrt{\frac{\tau}{\pi}}\, \xi\left(5\xi + \frac{1}{2}\xi^2 \right) e^{-\frac{\xi^2}{4\tau}},$$

and ξ is a dummy variable and f_1 and f_2 are the dummy functions and erfc $(.)$ is the complementary error function.

2.1 Solution when Schmidt number Sc=1

The solution for the velocity by equation (23) is not valid for $Sc = 1$. Since the Schmidt number is a measure of the relative importance of the viscosity and mass diffusivity of the fluid, the case $Sc = 1$ corresponds to those fluids whose momentum and concentration boundary layer thicknesses are of the same order of magnitude. Therefore, the solution for the velocity field when $Sc = 1$ has to be obtained separately from equations (9)-(11) subject to the initial and boundary conditions (12) and given by

$$u_1(\eta,\tau) = \frac{Gr}{\alpha - 1} \sum_{n=0}^{\infty} \left[f_2(a,\tau) - f_2(b,\tau) - f_2(a\sqrt{\alpha},\tau) - f_2(b\sqrt{\alpha},\tau) \right]$$
$$+ \frac{1}{2} Gc\eta \sum_{n=0}^{\infty} \left[f_3(a,\tau) - f_3(b,\tau) \right], \tag{25}$$

where

$$f_3(\xi,\tau) = \frac{1}{3} \sqrt{\frac{\tau}{\pi}} \left(4\tau + \xi^2 \right) e^{-\frac{\xi^2}{4\tau}} - \xi \left(\tau + \frac{1}{6} \xi^2 \right) erfc \left(\frac{\xi}{2\sqrt{\tau}} \right) \tag{26}$$

and f_3 is the dummy function and f_2 is given by (24).

3. Results and Discussions

In order to obtain the clear vision of the physical problem, a parametric study is performed and the obtained numerical results are displayed graphically. In Figs. 2-11, We have presented the non-dimensional fluid velocity u_1 and the fluid temperature θ for several values of radiation parameter R, Grashof number Gr, mass Grashof number Gc, Prandtl number Pr, Schmidt number Sc and time τ. The values of Schmidt number are chosen to represent the presence of species by hydrogen (0.24), water vapor (0.62), ammonia (0.78) and carbon dioxide (0.96) at temperature 25^oC and the pressure 1atmosphere. The values of Pr are chosen 0.72 and 7.1 for air and water, respectively, at temperature 20^oC and pressure 1 atm.. The values of radiation parameter and the chemical reaction parameter are chosen arbitrarily. It is revealed in Fig. 2 that the absolute value of the fluid velocity u_1 increases with an increase in the radiation parameter R. It is clearly seen that the velocity decreases with increasing value of R, i.e. the larger value of R is causedthe thicker the
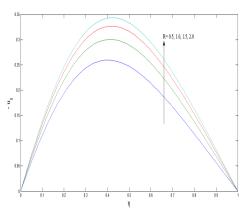

Fig. 2: Velocity profiles u_1 for different R when $Gr = 5$, $Gc = 3$, $Pr = 0.72$, $Sc = 0.96$ and $\tau = 0.5$

momentum boundary layer size. This is because an increase in R is caused an increase in the Rosseland mean radiation absorption coefficient k^* for fixed σ and T_h. It is also clear that the radiation has significant effect on the fluid velocity profiles in the presence of variable temperature and mass diffusion. The influence of the thermal Grashof number Gr on the fluid velocity u_1 is evident from Fig. 3. It can be observed that the the absolute value of fluid velocity u_1 increases for the increasing values of Gr. It is true physically as the thermal Grashof number Gr describes the ratio of bouyancy forces to viscous forces. Therefore, an increase in the values of Gr leads to increase in buoyancy forces, consequently the fluid velocity increases. Here the thermal Grashof number represents the effect of free convection currents. Physically, $Gr > 0$ means the heating of the cooling fluid of the boundary surface, $Gr < 0$ means the cooling of the heating fluid of the boundary surface and $Gr = 0$ corresponds the absence of free
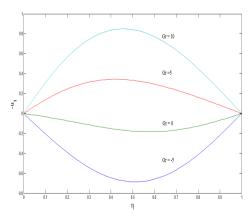

Fig. 3: Velocity profiles u_1 for different Gr when

$R = 2$, $Gc = 3$, $Pr = 0.72$, $Sc = 0.96$ and $\tau = 0.5$ convection current. It is also noticed from Fig. 3 that there is a reverse type of flow in the vertical channel for small values of Gr. Fig. 4 shows that the absolute value of the fluid velocity u_1 decreases for the increasing values of mass Grashof number Gc. This means that the mass buoyancy force opposes the fluid flow in the vertical channel in the presence of variable mass diffusion. Fig. 5 shows that the absolute value of the fluid velocity u_1 decreases with an increase in the Prandtl number Pr. Physically, it is true as the Prandtl number describes the ratio between momentum diffusivity and thermal diffusivity and hence controls the relative thickness of the momentum and the thermal boundary layers. As Pr increases the viscous forces (momentum diffusivity) dominate the thermal diffusivity consequently decreases the fluid velocity. The values of Schmidt number Sc were chosen to be $Sc = 0.45$, 0.62, 0.78 and 0.96, that represent the most common

diffusing chemical species . It is seen from Fig. 6 that the absolute value of the fluid velocity u_1 decreases with an increase in Schimdt number Sc. The physics of this observation is that the increased Schmidt number decreases the molecular diffusivityof the chemical species, which reduces the fluid velocity finally. Also, an increase of Sc (a predominance of the diffusive transport of momentum over that of mass) represents an increase in the momentum boundary layer thickness with a fixed species diffusivity and this causes the decrease in fluid velocity. Fig. 7 reveals that the absolute value of the fluid velocity u_1 increases near plate and it oscillates away from the plate with an increase in time τ. It is observed from Fig. 7 that as time increases, the absolute value of the fluid velocity in the vertical channel accelerates the upward direction. This is due to increasing buoyancy effects in the vertical channel with time increasing.
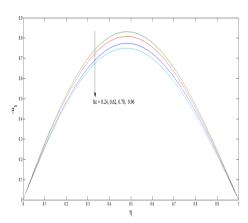

Fig. 4: Velocity profiles u_1 for different Gc when $Gr = 5$, $R = 2$, $Pr = 0.72$, $Sc = 0.96$ and $\tau = 0.5$

Fig. 6: Velocity profiles u_1 for different Sc when $Gr = 5$, $Gc = 3$, $Pr = 0.72$, $R = 2$ and $\tau = 0.5$

Fig. 5: Velocity profiles u_1 for different Pr when $Gr = 5$, $Gc = 3$, $R = 2$, $Sc = 0.96$ and $\tau = 0.5$
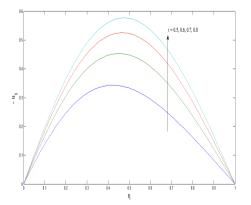

Fig. 7: Velocity profiles u_1 for different τ when $Gr = 5$, $Gc = 3$, $Pr = 0.72$, $Sc = 0.96$ and $R = 2$

The temperature variations are presented in Figs. 8-10 for different values of the radiation parameter R, Prandtl number Pr and time. It is seen from Fig. 8 that the fluid temperature decreases with an increase in radiation parameter R. This is in agreement with thisfact that radiation provides an additional means to diffuse energy. From the definition of R, an increase in the value of R implies to decreasing the radiation effects. In the presence of radiation, the thermal boundary layer always found to thicken which implies that the radiation provides an additional means to diffuse energy. This means that the thermal boundary layer decreases and there is more uniform temperature distribution across the boundary layer. Fig. 9 shows that the fluid temperature θ decreases with an increase in Prandtl number Pr. The reason is that smaller values of Pr are equivalent to increase in the thermal conductivity of the fluid and therefore, the heat is able to diffuse away from the heated surface more rapidly for higher values Pr. Hence in the case of smaller Prandtl numbers the
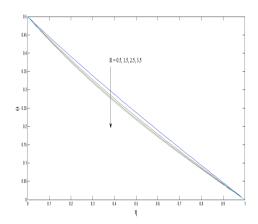

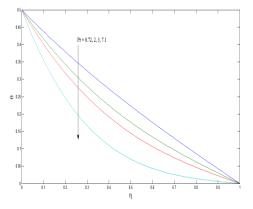Fig. 8: Temperature profiles for different R when $Pr = 0.72$ and $\tau = 0.5$

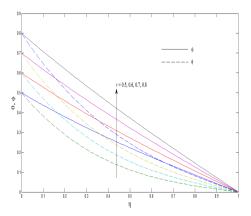Fig. 9: Temperature profiles for different Pr when $R = 2$ and $\tau = 0.5$

Fig. 10: Temperature profiles for different τ when $Pr = 0.72$, $Sc = 0.96$ and $R = 2$
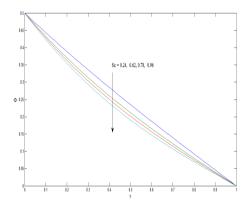

Fig. 11: Concentration profiles for different Sc when $\tau = 0.5$

thermal boundary layer is thicker and the heat transfer is reduced. The temperature and mass concentration profiles for different values of time τ are presented in Fig. 10. It is observed that these profiles increase in the vertical channel as time τ increases. It is seen from Fig. 11 that the concentration profiles increase with an increase in Schimdt number Sc. As expected, if all other physical parameters are kept constant, the mass transfer decreases as Sc increases, i.e. an increase in the value of the Schmidt number Sc is associated with a decrease in the concentration profiles. Further, it may be observed from this figure that the effect of Schmidt number Sc on concentration distribution slowly decreases in the concentration boundary layer for higher values of Sc.

The heat and mass transfer rates at the plates $\eta = 0,1$ are, respectively given by

$$\theta'(0,\tau) = 2\sqrt{\alpha}\sum_{n=0}^{\infty}\left[G_1(c\sqrt{\alpha},\tau) - G_1(d\sqrt{\alpha},\tau)\right] \quad (27)$$

$$\theta^{'}(1,\tau) = 2\sqrt{\alpha}\sum_{n=0}^{\infty} H_1(e\sqrt{\alpha},\tau), \qquad (28)$$

$$\phi^{'}(0,\tau) = 2\sqrt{Sc}\sum_{n=0}^{\infty}\Big[G_1(c\sqrt{Sc},\tau) - G_1(d\sqrt{Sc},\tau)\Big] \qquad (29)$$

$$\phi^{'}(1,\tau) = 2\sqrt{Sc}\sum_{n=0}^{\infty} H_1(e\sqrt{Sc},\tau), \qquad (30)$$

where

$$G_1(\xi,\tau) = \xi\, erfc\left(\frac{\xi}{\sqrt{\tau}}\right) - \sqrt{\frac{\tau}{\pi}}\, e^{-\frac{\xi^2}{\tau}},$$

$$H_1(\xi,\tau) = \xi\, erfc\left(\frac{\xi}{2\sqrt{\tau}}\right) - \sqrt{\frac{\tau}{\pi}}\, e^{-\frac{\xi^2}{4\tau}} \qquad (31)$$

and $c = n$, $d = n+1$ and $e = 2n+1$

The Numerical results of the heat transfer rate $-\theta^{'}(0,\tau)$ and $\theta^{'}(1,\tau)$ at the plates $\eta = 0,1$ for several values of radiation parameter R, Prandtl number Pr and time τ are presented in Figs. 12-13. It is observed from Figs. 12-13 that the heat transfer rates $-\theta^{'}(0,\tau)$ and $\theta^{'}(1,\tau)$ increase with an increase in either radiation parameter R or Prandtl number Pr or time τ. This may be explained by the fact that frictional forces become dominant by increasing the values of Prandtl number Pr and hence yield the greater heat transfer rate. An increase in Prandtl number reduces the thermal boundary layer thickness. The Prandtl number signifies the ratio of momentum diffusivity to thermal diffusivity. The Fluids with lower Prandtl number will have the higher thermal conductivities so that the heat can diffuse from the plate faster than thefluids with higher Pr (thinner boundary layers). Hence, Prandtl number can be used to increase the cooling rate in conducting flows. It is clear that the heat transfer rate is more in the presence of thermal radiation. The negative value
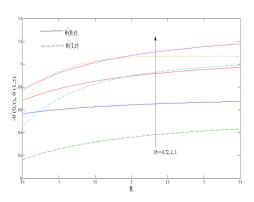

Fig. 12: Rate of heat transfer $\theta^{'}(0,\tau)$ and $\theta^{'}(1,\tau)$ for Pr when $\tau = 0.5$
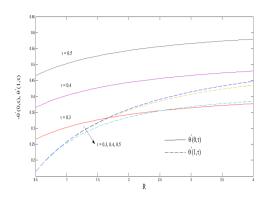

Fig. 13: The heat transfer Rate $\theta^{'}(0,\tau)$ and $\theta^{'}(1,\tau)$ for τ when $Pr = 0.71$
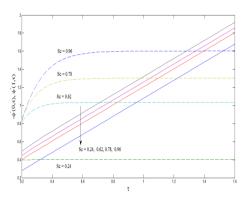

Fig. 14:The mass transfer $\phi^{'}(0,\tau)$ and $\phi^{'}(1,\tau)$

of $\theta^{'}(0,\tau)$ explains physically that there is the heat flow from the hot plate $\eta = 0$ to the ambient fluid. It is observed from Fig. 14 that the mass transfer rate $-\phi^{'}(0,\tau)$ decreases while $\phi^{'}(1,\tau)$ increases with an increase in either Schmidt number Sc or time τ.

From an engineering point of view, the most important characteristic of the flow is the shear stresses at the plate $\eta = 0,1$ that are, respectively given by

$$\tau_{x_0} = \left(\frac{\partial u_1}{\partial \eta}\right)_{\eta=0}$$

$$= \begin{cases} 2\dfrac{Gr(Sc-1)+Gc(\alpha-1)}{(\alpha-1)(Sc-1)}\sum_{n=0}^{\infty}\big[G_2(c,\tau)+G_2(b,\tau)\big] \\[4pt] -2\dfrac{Gr\sqrt{\alpha}}{\alpha-1}\sum_{n=0}^{\infty}\big[G_2(c\sqrt{\alpha},\tau)+G_2(d\sqrt{\alpha},\tau)\big] \\[4pt] -2\dfrac{Gc\sqrt{Sc}}{Sc-1}\sum_{n=0}^{\infty}\big[G_2(c\sqrt{Sc},\tau)+G_2(d\sqrt{Sc},\tau)\big] \quad \text{for } Sc \neq 1 \\[10pt] \dfrac{2Gr}{\alpha-1}\sum_{n=0}^{\infty}[G_2(c,\tau)+G_2(d,\tau)-\sqrt{\alpha}\{G_2(n\sqrt{\alpha},\tau)+G_2(d\sqrt{\alpha},\tau)\}] \\[4pt] +Gc\sum_{n=0}^{\infty}\big[G_2(c,\tau)+G_2(d,\tau)\big] \qquad\qquad \text{for } Sc = 1 \end{cases}$$

$$\tau_{x_1} = \left(\frac{\partial u_1}{\partial \eta}\right)_{\eta=1}$$

$$
= \begin{cases} 2\dfrac{Gr(Sc-1)+Gc(\alpha-1)}{(\alpha-1)(Sc-1)}\sum_{n=0}^{\infty}H_2(e,\tau) \\[2mm] -2\dfrac{Gr\sqrt{\alpha}}{\alpha-1}\sum_{n=0}^{\infty}H_2(e\sqrt{\alpha},\tau)-2\dfrac{Gc\sqrt{Sc}}{Sc-1}\sum_{n=0}^{\infty}H_2(e\sqrt{Sc},\tau) \quad \text{for } Sc\neq 1 \\[3mm] 2\dfrac{Gr\sqrt{\alpha}}{\alpha-1}\sum_{n=0}^{\infty}\left[H_2(e,\tau)-\sqrt{\alpha}H_2(e\sqrt{\alpha},\tau)\right]+2\sum_{n=0}^{\infty}H_3(e,\tau) \quad \text{for } Sc=1 \end{cases}
$$

where

$$
G_2(\xi,\tau)=\xi\left(\tau+\frac{1}{3}\xi\right)erfc\left(\frac{\xi}{\sqrt{\tau}}\right)-\frac{2}{3}\sqrt{\frac{\tau}{\pi}}\left(\tau+\xi^2\right)e^{-\frac{\xi^2}{\tau}},
$$

$$
H_2(\xi,\tau)=\xi\left(2\tau+\frac{1}{3}\xi\right)erfc\left(\frac{\xi}{2\sqrt{\tau}}\right)-\frac{2}{3}\sqrt{\frac{\tau}{\pi}}\left(4\tau+\xi^2\right)e^{-\frac{\xi^2}{4\tau}}
$$

(34)

The Numerical values of the non-dimensional shear stress at the plates $\eta=0,1$ are presented in Figs. 15-19 for several values of thermal Grashof number Gr, mass Grashof number Gc, radiation parameter R, Prandtl number Pr and time τ. Figs. 15-16 show that the shear stresses τ_{x_0} and τ_{x_1} increase with an increase in either thermal Grashof number Gr or mass Grashof number Gc. Fig. 17 reveals that the shear stresses τ_{x_0} and τ_{x_1} reduce for increasing values of Schmidt number Sc. Physically, it is true since an increase in Sc serves to decrease momentum boundary layer thickness. It is seen from Fig. 18 that the shear stress τ_{x_0} reduces while the shear stresses τ_{x_1} increases with an increase in Prandtl number Pr. It is observed that an increase in the Prandtl number results in a decrease of the thermal boundary layer thickness and in general lower average temperature within the boundary layer. The reason is that smaller values of Pr are equivalent to increase in the thermal conductivity of the fluid and therefore, the heat is able to diffuse away from the heated surface more rapidly for higher values of Pr. Hence, in the case of smaller Prandtl number as the
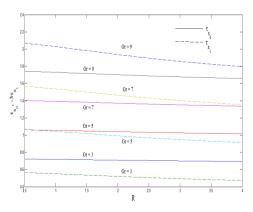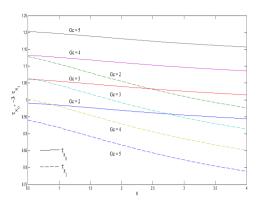

Fig. 16: Shear stresses τ_{x_0} and τ_{x_1} for Gc when $Gr=5$, $Sc=0.96$, $Pr=0.71$ and $\tau=0.5$

thermal boundary layer is thicker and the rate of hear transfer is reduced. Fig. 17 shows that the shear stresses τ_{x_0} and τ_{x_1} increase as time τ increases. It is also seen that the shear stresses τ_{x_0} and τ_{x_1} reduce with increasing values of radiation parameter R.
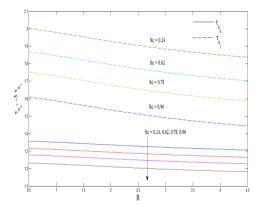

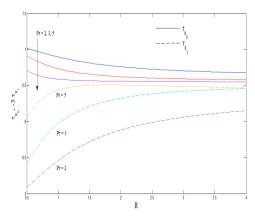Fig. 17: Shear stresses τ_{x_0} and τ_{x_1} for Sc when $Gr=5$, $Gc=3$, $Pr=0.71$ and $\tau=0.5$

Fig. 18: Shear stresses τ_{x_0} and τ_{x_1} for Pr when $Gr=5$, $Sc=2.62$, $Gc=3$ and $\tau=0.5$

Fig. 15: Shear stresses τ_{x_0} and τ_{x_1} for Gr when $Gc=3$, $Sc=0.96$, $Pr=0.71$ and $\tau=0.5$

Fig. 19: Shear stresses τ_{x_0} and τ_{x_1} for time τ when $Gr = 5$, $Sc = 0.96$, $Pr = 0.72$ and $Gc = 3$

4. Conclusion

The Exact solutions for the unsteady free convection flow of an optically dense incompressible viscous fluid between two long vertical parallel plates with variable temperature and mass diffusion in the presence of thermal radiation have been obtained by using the Laplace transform technique. The effects of the pertinent parameters such as the radiation parameter, buoyancy forces, Schmidt number and time on the fluid velocity and temperature fields and shear stresses at the plate have been studied in detail. The study shows that these parameters have significant impact on the velocity, temperature, mass concentration and the shear stresses at the plates. The following conclusions are extracted from this study:

- An increase in the radiation parameter leads to a decrease in the fluid velocity as well as the temperature.
- The fluid velocity and temperature decrease with an increase in the Prandtl number.
- The fluid velocity increases with increases in the Grashof number and an increase in time leads to increases in the fluid velocity, temperature and concentration.
- It is expected that the results of this study will be served as a mechanism to develop the design of cooling and energy systems and nuclear thermo-hydraulics.

References

[1]. Cussler, E. L. (1998). Diffusion Mass Transfer in Fluid Systems, Cambridge University Press, Cambridge, UK.

[2]. Lee, T.S., Parikh, P.G., Acrivos, A., Bershadar, D. (1982). Natural convection in a vertical channel with opposing buoyancy forces. Int J Heat Mass Transf 25(4), 499-511.

[3]. Yan, W.M., Lin, T.F., Chang, C.J. (1988). Combined heat and mass transfer in natural convection vertical parallel plates. Warme-Stoffübertrag 23,69-76.

[4]. Nelson, D.J., Wood, B.D. (1989). Combined heat and mass transfer natural convection between vertical parallel plates. Int. J. Heat Mass Transf. 32(9), 1779-1787.

[5]. Nelson, D.J., Wood, B.D. (1989). Fully developed combined heat and mass transfer natural convection between vertical parallel plates with asymmetric boundary conditions. Int. J. Heat Mass Transf. 32, 1789-1792.

[6]. Yan, W.M., Lin, T.F. (1990). Combined heat and mass transfer natural convection between vertical parallel plates with film evaporation. Int J Heat Mass Transf 33(3), 529-541.

[7]. Yan, W.M., Lin, T.F. (1991). Evaporative cooling of liquid film through interfacial heat and mass transfer in a vertical channel - II. Numerical study. Int J Heat Mass Transf 34(4-5), 1113-1124.

[8]. Yan, W.M., Lin, T.F. (1991). Evaporative cooling of liquid film through interfacial heat and mass transfer in a vertical channel - I. Experimental study. Int. J. Heat Mass Transf. 34(4-5), 1105-1111.

[9]. Desrayaud, G., Lauriat, G. (2001). Heat and mass transfer analogy for condensation of humid air in vertical channel. Heat Mass Transf. 37, 67-76.

[10]. Salah El-Din, M.M. (2003). Effect of thermal and mass buoyancy forces on the development of laminar mixed convection between vertical parallel plates with uniform wall heat and mass fluxes. Int. J. Therm. Sci. 42, 447-453.

[11]. Cheng, C-Y. (2006). Fully developed natural convection heat and mass transfer of a micropolar fluid in a vertical channel with asymmetric wall temperatures and concentrations. Int Commun. Heat Mass Transf. 33,627-635.

[12]. Narahari, M. (2008). Transient free convection flow between two long vertical parallel plates with constant temperature and mass diffusion. In: Proceedings of the world congress on engineering 2008, vol II, WEC 2008, July 2-4, London, UK, pp 1614-1619

[13]. Rosseland, S. (1936). Theoretical Astrophysics, Oxford University, New York, NY, USA.